



Performance and testing of glass-ceramic sealant used to join anode-supported-electrolyte to Crofer22APU in planar solid oxide fuel cells

F. Smeacetto^{a,*}, A. Chrysanthou^b, M. Salvo^a, Z. Zhang^b, M. Ferraris^a

^a Department of Materials Science and Chemical Engineering, Politecnico di Torino, Corso Duca degli Abruzzi 24, 10129 Torino, Italy

^b School of Aerospace, Automotive and Design Engineering, University of Hertfordshire, College Lane, Hatfield, Herts AL10 9AB, UK

ARTICLE INFO

Article history:

Received 16 October 2008

Received in revised form

22 December 2008

Accepted 18 January 2009

Available online 15 February 2009

Keywords:

Glass-ceramic

Fuel cell

Sealant

Hydrogen

Crofer22APU

ABSTRACT

This work describes the performance and testing of a glass-ceramic sealant used to join the ceramic electrolyte (anode-supported-electrolyte (ASE)) to the metallic interconnect (Crofer22APU) in planar SOFC stacks. The designed glass-ceramic sealant is a barium and boron free silica-based glass, which crystallizes by means of the heat-treatment after being deposited on substrates by the slurry technique.

Joined ASE/glass-ceramic seal/Crofer22APU samples were tested for 500 h in H₂–3H₂O atmosphere at the fuel cell operating temperature of 800 °C.

Moreover, the joined ASE/glass-ceramic seal/Crofer22APU samples were submitted to three thermal cycles each of 120 h duration, in order to evaluate the thermomechanical stability of the sealant.

The microstructures and elemental distribution at Crofer22APU/glass-ceramic and ASE/glass-ceramic interfaces were investigated.

SEM micrograph observations of joined samples that underwent cyclic thermal tests and exposure for 500 h in H₂–3H₂O atmosphere showed that the adhesion between the glass-ceramic and Crofer22APU at either interface was very good and no microstructural changes were detected at the interfacial boundaries.

The study showed that the use of the glass-ceramic was successful in preventing strong adverse corrosion effects at the Crofer22APU/glass-ceramic sealant interface.

© 2009 Elsevier B.V. All rights reserved.

1. Introduction

Solid oxide fuel cells (SOFCs) are highly efficient energy conversion devices which produce electricity by the electrochemical reaction between a fuel and an oxidant. Among the different SOFCs, the planar type, which is expected to be cost effective and mechanically robust, offers an attractive potential for increased power densities compared to other concepts. A fuel cell device consists of an anode electrode (exposed to fuel), an electrolyte, and a cathode electrode (exposed to oxidant) [1,2].

The repeating unit of a planar solid oxide fuel cell (SOFC) is formed by anode–electrolyte–cathode and interconnects. The interconnect links the anode of one cell to the cathode of the neighbouring cell [3]. In most SOFC stack designs, the interconnect is sealed to the ceramic cell components [4]. A promising interconnect material is chromia-forming ferritic stainless steel. However, the seal between the stainless steel metal interconnect and the ceramic SOFC components presents a challenge [5,6].

The sealants for planar SOFCs must meet some important requirements: they have to be hermetic in order to prevent mixing of the fuel and oxidant and should have a thermal expansion coefficient close to those of the interconnect and the electrolyte. Moreover, the sealant must be mechanically and thermochemically stable in both oxidizing and wet-reducing environments at 800 °C and must not undergo any reaction with the other cell components. The problem becomes even more challenging as there is also a requirement for thermal cycle stability for planar stacks in which dissimilar SOFC components are sealed together. The sealants have to survive for several hundreds of thermal cycles during SOFC operations. Any cracks that form in the sealants or at the interfacial regions can cause leakage that leads to lower cell performance and efficiency. A number of different approaches are currently being studied for sealing SOFCs including [7]: brazing [8–10], compressive seals, as well as glasses, glass-ceramic seals and glass-composite seals [11–19].

Glass-ceramics can be prepared by controlled sintering and crystallization of glasses and have superior mechanical properties and higher viscosity at the SOFC operating temperature than glasses. Furthermore, they can have thermal expansion coefficients very different from the parent glass, due to the different crystalline phases

* Corresponding author. Tel.: +39 011564706; fax: +39 0115644699.

E-mail address: federico.smeacetto@polito.it (F. Smeacetto).

that form and their relative proportion. Glass-ceramics show better resistance to the severe service environment (both oxidizing and reducing) than brazing alloys, and by carefully choosing the glass composition, they can meet most of the requirements that need to be exhibited by the ideal sealant material.

In order to develop a suitable glass-ceramic sealant, it is therefore necessary to understand the crystallization kinetics, the sealing properties and the chemical interactions with other components of the cell. Barium aluminosilicate sealants have shown high reactivity with the metallic interconnect at 800–900 °C forming a porous and weak interface composed of barium chromate (BaCrO_4) and monocelsian ($\text{BaAl}_2\text{Si}_2\text{O}_8$), while borate glasses are not sufficiently stable in a humidified fuel gas environment [20,21].

Moreover, glass-ceramic seals have good hermeticity and are thermally and environmentally stable. However, the inherent brittleness of glasses may cause cracks to develop in seals during thermal cycling or thermal shock. This can cause leakage that would lead to lower cell performance and efficiency.

Owing to these problems that have been observed for barium aluminosilicate sealants, the authors have developed an alternative sealant based on a sodium–calcium–aluminosilicate glass-ceramic [22] consisting of gehlenite ($\text{Ca}_2\text{Al}_2\text{SiO}_7$) and a sodium aluminosilicate (NaAlSiO_4) phase. In the study that is presented here, the testing and performance of the sodium–calcium–aluminosilicate glass-ceramic sealant that was used to join the Anode-supported-electrolyte to Crofer22APU in planar SOFCs are reported. The investigation involved static treatments in humidified hydrogen and thermal cycling in air for 500 h; this can be considered as a preliminary screening on the glass-ceramic sealant performance, taking in account that the target operational life of the cell should be thousand of h (e.g., 10 kh).

2. Experimental

The heat resistant metal alloy used for this study was Crofer22APU (Cr 20–24, C 0.03, Mn 0.30–0.80, Si 0.50, Fe balance, wt.%) manufactured by Tyssen Krupp, Germany and supplied by HT Ceramix, Switzerland). The Crofer22APU was preoxidised as described in Ref. [22]. The anode-supported-electrolyte (ASE) (electrolyte: cubic zirconia, 8 mol% YSZ; anode: NiO–YSZ) was supplied by HT Ceramix (Switzerland). The Crofer22APU, and ASE samples to be joined were cut to obtain a final joined sample measuring 6 mm × 6 mm × 2 mm.

The melting procedure, thermal and thermomechanical characterization of the sealant (labeled as SACN) are described elsewhere [22,23].

The sealant composition ranged between 53 and 58 mol% SiO_2 , 16–18 mol% Al_2O_3 , 24–26 mol% CaO and 10–12 mol% Na_2O . The T_g at 670 °C and $T_{\text{softening}}$ at 740 °C were measured by differential thermal analysis (DTA), while two crystallization temperatures were detected at 830 and 940 °C, respectively. Two crystalline phases were detected by X-ray diffraction (XRD) in the glass-ceramic obtained after the sealant heat-treatment necessary for the joining process: $\text{Ca}_2\text{Al}_2\text{SiO}_7$ and NaAlSiO_4 .

The joints were obtained by placing the Crofer22APU plates on the yttria-stabilised zirconia (YSZ) surface of the anode-supported-electrolyte with the SACN slurry sandwiched in between. The slurry was made of a mixture of glass powder ($38 < \mu\text{m} < 75$) dispersed in ethanol (solid content 40 wt.%).

Heat-treatments were performed in a tubular oven (Ar atmosphere) at a temperature above the glass softening point, without applying any load. Reproducible results, in terms of joint thickness and homogeneity were obtained. The joining thermal treatment was carried out from room temperature to 900 °C, with a heat-

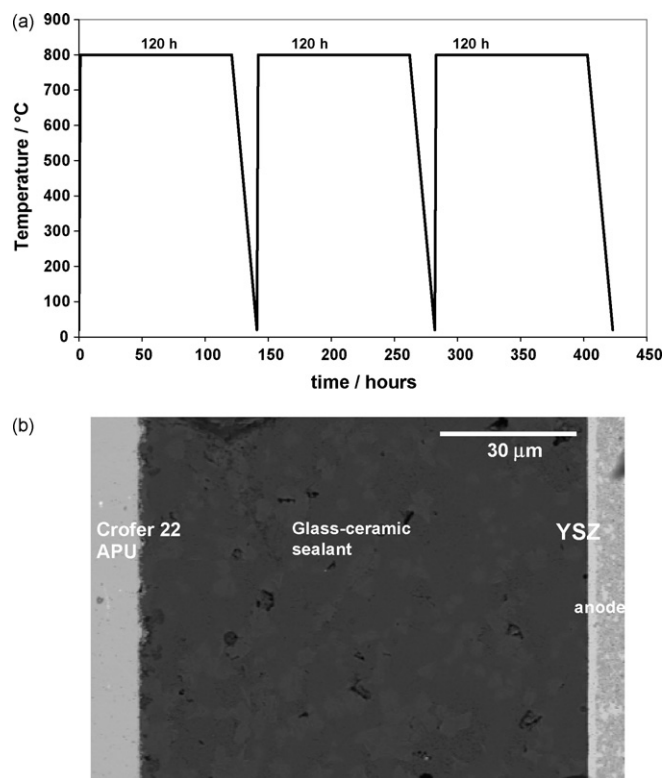


Fig. 1. (a) Thermal cycles of Crofer22APU/SACN/ASE samples; (b) Crofer22APU/glass-ceramic sealant/ASE SEM cross-section after multiple thermal cycles tests (RT–800 °C).

ing rate of 5 °C min⁻¹ and a dwelling time of 30 min at 900 °C; the cooling rate was 5 °C min⁻¹.

Some Crofer22APU/SACN/ASE samples were exposed to H_2 –3 H_2O atmosphere at 800 °C for 500 h. Details of the experimental apparatus are reported in Ref. [23].

Thermal cycles of Crofer22APU/SACN/ASE samples were performed in a muffle furnace with static air from room temperature to 800 ± 20 °C for a period of 400 h. This involved heating to 800 ± 20 °C and dwelling for 120 h for three cycles, each with an interval of 20 h between them. During each 20 h interval the samples were allowed to cool down slowly down (5 °C min⁻¹) to room temperature inside the furnace. The thermal cycles are schematically represented in Fig. 1a.

Cross-sections of joined samples were characterized by scanning electron microscopy (SEM) (FEI Inspect, Philips 525 M and JEOL 6390LV) after polishing. EDS (SW9100 EDAX) analysis was carried out in order to detect any elemental diffusion into or away from the seal after H_2 –3% H_2O atmosphere exposure and following thermal cycling at 800 °C and to examine for any chemical interactions between Crofer22APU and ASE with the glass-ceramic sealant at the three-phase boundary under reducing and oxidizing conditions.

3. Results and discussion

3.1. Crofer22APU/glass-ceramic sealant/ASE joined samples after multiple thermal cycles (RT–800 °C)

Fig. 1b shows a cross-section of a Crofer22/glass-ceramic sealant/ASE joined sample after three thermal cycles each of 120 h at 800 °C with slow cooling intervals to room temperature of 20 h, according to Fig. 1a. It can be observed that the adhesion between the glass-ceramic and Crofer22 and YSZ is still sound and that no cracks are detected in the glass-ceramic sealant. Fig. 2a and b show

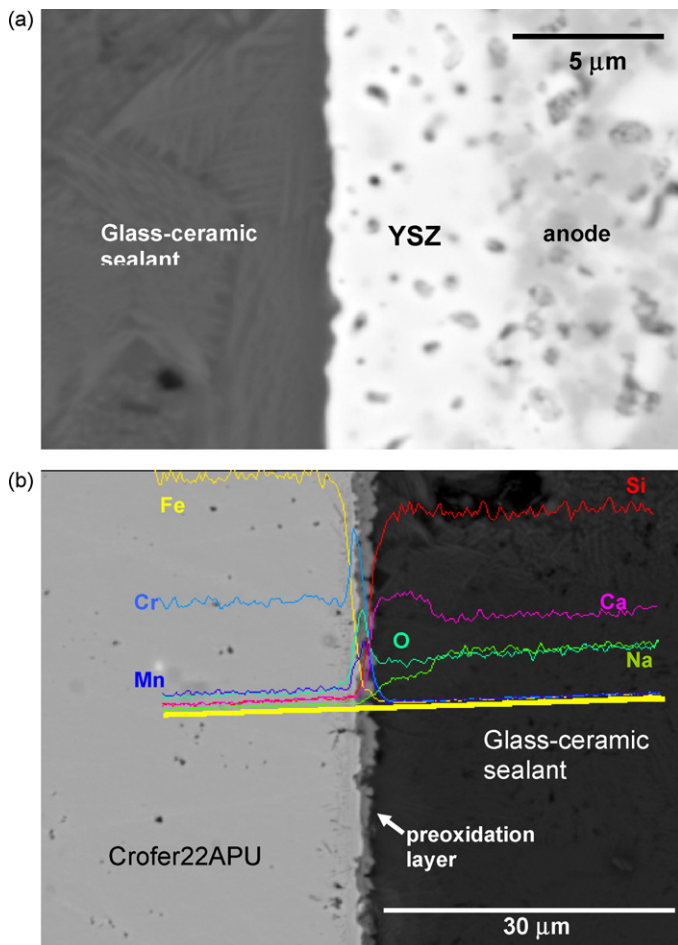


Fig. 2. (a) SEM cross-section of the interface zone between the glass-ceramic and the YSZ side of ASE in Crofer22APU/glass-ceramic sealant/ASE joined sample after multiple thermal cycles tests (RT–800 °C); (b) Crofer22APU/glass-ceramic interface and elements line scan after multiple thermal cycles tests (RT–800 °C).

micrographs of the glass-ceramic/ASE and Crofer22/glass-ceramic interface, respectively. In Fig. 2a it can be observed that the very thin YSZ electrolyte (5 μm) is not cracked, while Fig. 2b shows that no interfacial delaminations occurred at the Crofer22/glass-ceramic sealant interface after thermal cycling. The results of the EDAX analysis did not reveal any significant changes after heat-treatment of the joint. Fig. 2b presents the EDS elemental line scans for Cr, Fe, Mn, O, Na, Ca and Si at the Crofer22/glass-ceramic sealant interface. According to the EDS analysis, the amounts of chromium and manganese in the preoxidation layer remained high as before exposure to air at 800 °C and there was no reactive interaction with the sealant. A preoxidation layer had been formed consisting of a chromia sub-layer and a chromium–manganese-rich spinel top layer [24]. The EDS results show that the same preoxidation layer was present after exposure to air at 800 °C (Fig. 2b). These results are in contrast to the observations of Ogasawara et al. [25] who used a sodium oxide-containing silicate sealant of different composition to the present work and reported that sodium chromates were formed at the Crofer22APU/glass-ceramic sealant interface, giving rise to chromium depletion at the interfacial area. The formation of the preoxidation layer of chromia and chromium–manganese oxide spinel is expected to be of great benefit because it can prevent or minimize chromia vapourisation under glass-ceramic sealant operating conditions. The results presented in Fig. 2b also indicate that during exposure to air there was no diffusion of iron into the chromia and the chromium–manganese oxide spinel phases.

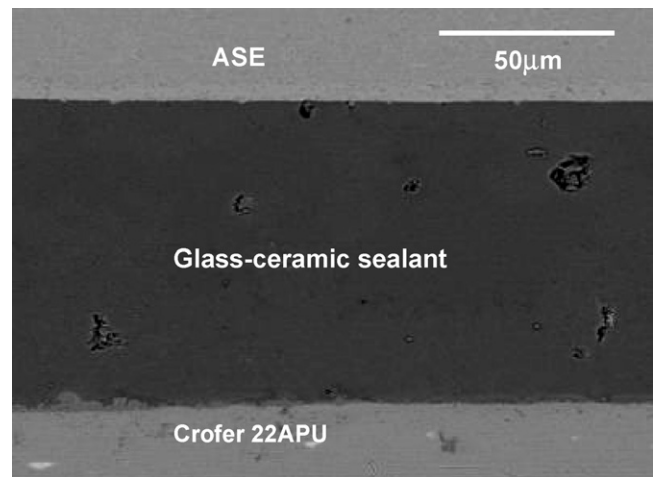


Fig. 3. Crofer22APU/glass-ceramic sealant/ASE SEM cross-section after 500 h in humidified hydrogen at 800 °C.

Concerning the thermal, physical and chemical stability of the sealant, it must be highlighted that XRD analysis revealed no change of crystalline phases ($\text{Ca}_2\text{Al}_2\text{SiO}_7$ and NaAlSiO_4) and no change in their XRD intensity (XRD patterns not reported here).

Moreover, the thermal expansion coefficient of the glass-ceramic sealant after 400 h at 800 °C was measured to be $10.7 \times$

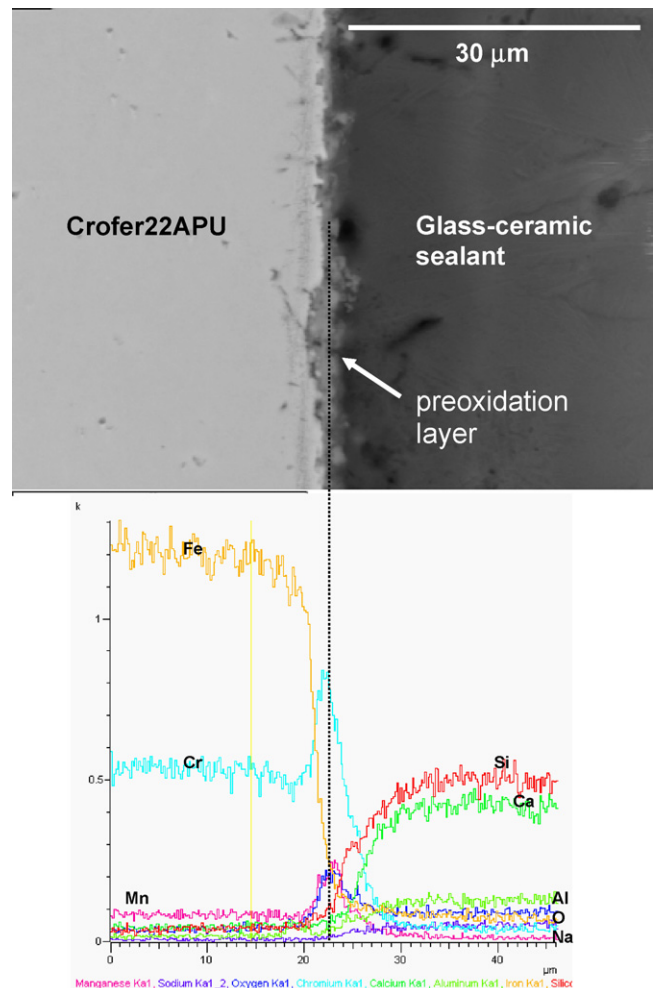


Fig. 4. Crofer22APU/glass-ceramic sealant SEM cross-section (after 500 h in humidified hydrogen at 800 °C) and relative elements line scan.

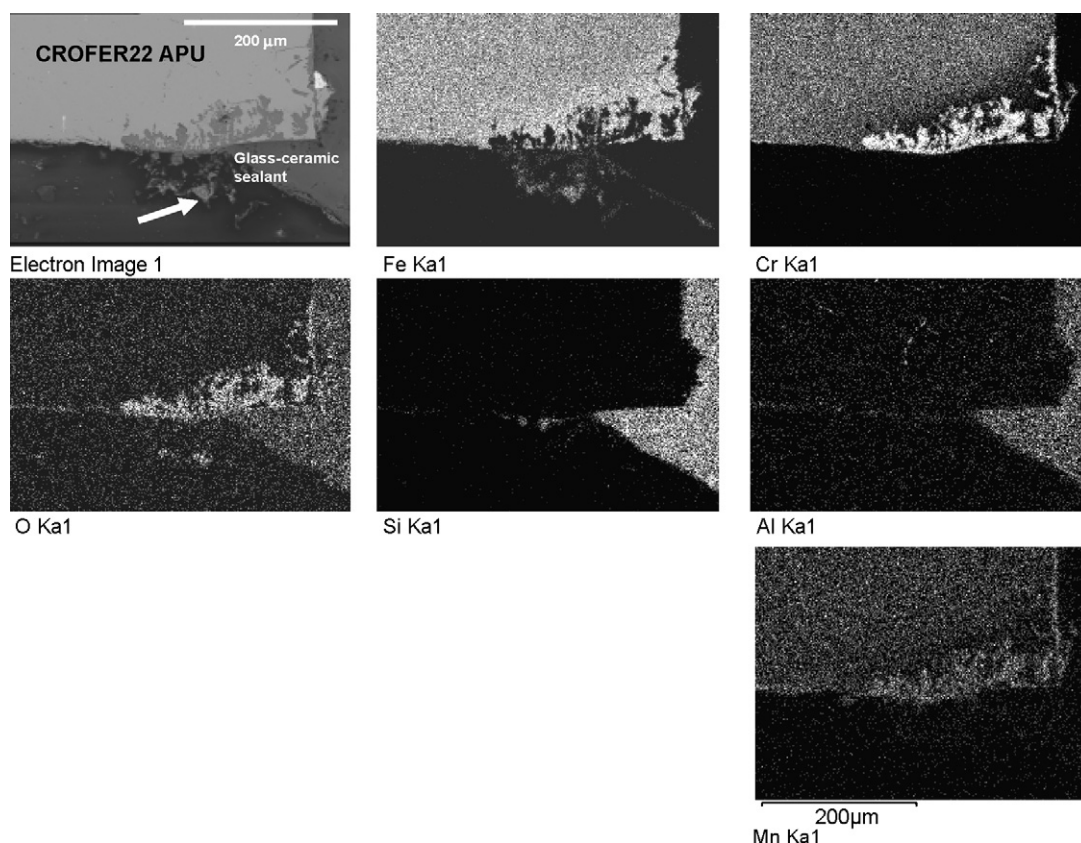


Fig. 5. The three-phase boundary zone (Crofer22APU-glass-ceramic in humidified hydrogen) and relative EDS elements mapping.

$10^{-6} \text{ } ^\circ\text{C}^{-1}$, which is the same value as for the glass-ceramic after the heat-treatment that it underwent during the joining process.

In addition, there were no microstructural changes following thermal cyclic treatment. It can therefore be concluded that no interfacial reactions took place and no microstructural changes were detected at the interfacial boundaries. The SEM investigation revealed no changes to adversely affect the adhesion at each interface.

3.2. Crofer22APU/glass-ceramic sealant/ASE joined samples after exposure to H_2 -3% H_2O atmosphere (500 h)

After a long-term exposure (500 h) at $800 \text{ } ^\circ\text{C}$ in a reducing atmosphere (H_2 -3% H_2O), it was observed that the seal region with an average thickness of $100 \text{ } \mu\text{m}$ remained intact. Fig. 3 shows a SEM micrograph of the cross-section of the Crofer22APU/glass-ceramic sealant/YSZ interfacial areas after 500 h exposure to the H_2 -3% H_2O atmosphere. The SEM micrograph is focused on the central part of the joined sample. It is evident that no interfacial delamination at the glass-ceramic sealant/steel and glass-ceramic sealant/YSZ interfaces took place. It can be also observed that the joint region does not exhibit any substantial modifications from the morphological point of view. No cracks or pores are present, and the interfaces between the glass-ceramic sealant and both Crofer22APU alloy and YSZ ceramic are continuous and free of cracks. Fig. 4 shows the EDS line scan and elemental distribution at the Crofer22APU/glass-ceramic sealant interface after 500 h exposure to the H_2 -3% H_2O atmosphere; it is evident that there is no reaction between the chromium-manganese oxide scale and the glass-ceramic components and consequently there are no new interfacial products at the interface. Moreover, it can be also observed that during the exposure to the humidified hydrogen, there was no diffusion of manganese to the oxide scale or to the glass-ceramic

from the Crofer22APU. The preoxidised oxide layer of chromia and chromium-manganese oxide spinel was present also before the exposure to humidified hydrogen. This observation is in agreement with previous work reported by Nielsen et al. [26].

The microstructure at the edges of the samples around the glass-ceramic sealant/Crofer22APU interface was also investigated in order to examine for the presence of any corrosion products. Fig. 5 shows a micrograph and elemental maps of the three-phase boundary zone (Crofer22APU-glass-ceramic sealant-humidified hydrogen). Internal oxidation of Cr and diffusion of Fe outwards can be observed in the elemental maps. The chromium-manganese oxide is adherent and generally continuous, but the iron oxide on the outer surface (see arrow in Fig. 5) does not adhere well and appears to cause some breakaway corrosion. This situation is probably due to the diffusion of iron to the outside. The iron oxide does not adhere well on the surface as some porosity is detected. Also there is a slight depletion of Cr and Mn just below the spinel layer and an increase in the amount of Fe. Such depletion in the amounts of chromium and manganese is undesirable as the oxide layer could not be self-healing in case of it becoming damaged. Using thermodynamic data compiled by Turkdogan [27], the partial pressure of oxygen in equilibrium with a 97% H_2 -3% H_2O gas mixture at $800 \text{ } ^\circ\text{C}$ was calculated to be $5.13 \times 10^{-22} \text{ atm}$. According to thermodynamic calculations using the same source [27], chromium will oxidize in environments where the partial pressure of oxygen exceeds $6.91 \times 10^{-28} \text{ atm}$ and therefore the conditions for chromium are oxidising as observed. According to the thermodynamic calculations, the oxygen partial pressure required to oxidize iron to wustite (FeO) at $800 \text{ } ^\circ\text{C}$ should exceed $1.71 \times 10^{-19} \text{ atm}$ at $800 \text{ } ^\circ\text{C}$. The partial pressure of oxygen is therefore lower than that which is required in order to oxidize iron to FeO . In spite of this a small amount of FeO has been observed to form at the three-phase interface only and to break away. It is not clear why the iron is oxidizing under

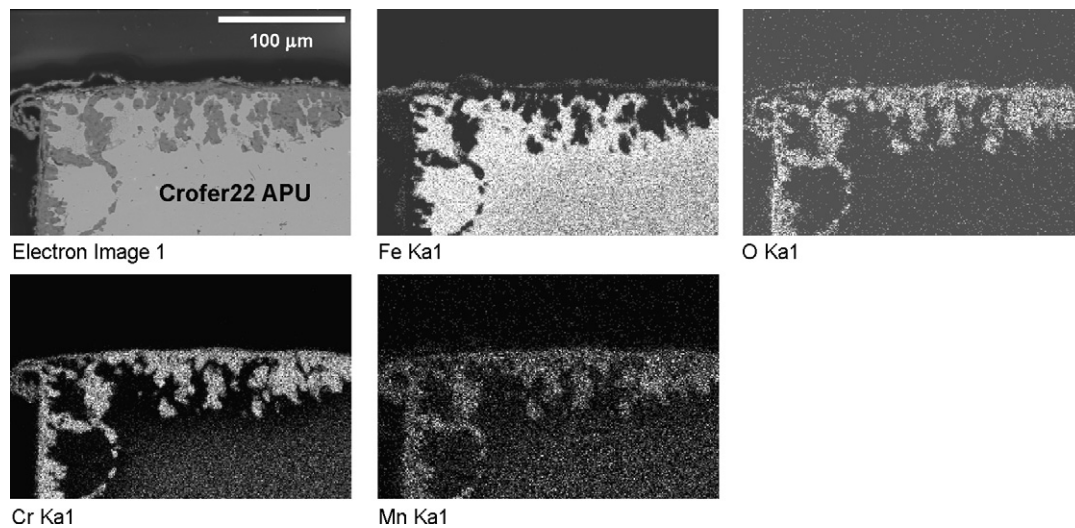


Fig. 6. Crofer22APU without the sealant at 800 °C for 500 h in H₂-3% H₂O.

these conditions. One possibility is that this may be due to localized formation of Cr(OH)₂ which is volatile. It has previously been reported by Essuman et al. [28] that small amounts of water vapour can cause the partial pressure of Cr(OH)₂ in equilibrium with Cr₂O₃ scale to exceed the partial pressure of CrO₃. The reactive evaporation of Cr₂O₃ scales becomes more pronounced as the water vapour in the gas increases. This observation in the behaviour of Cr₂O₃ is a possible means that can give rise to exposure of the iron. However, the results of the SEM examination do not seem to support localized

formation and evaporation of Cr(OH)₂. Even if Cr(OH)₂ formation were to take place, it is not clear as to why the iron, contrary to thermodynamic predictions, should undergo oxidation under the conditions used in the present study. Oxidation of the iron by reaction with the oxides in the sealant is highly unlikely as the oxides in the sealant are thermodynamically more stable than the oxides of iron. Further investigation was then carried out on the unexpected oxidation of iron by heat-treating the Crofer22 stainless steel on its own without the sealant at 800 °C for 500 h in H₂-3% H₂O. Examina-

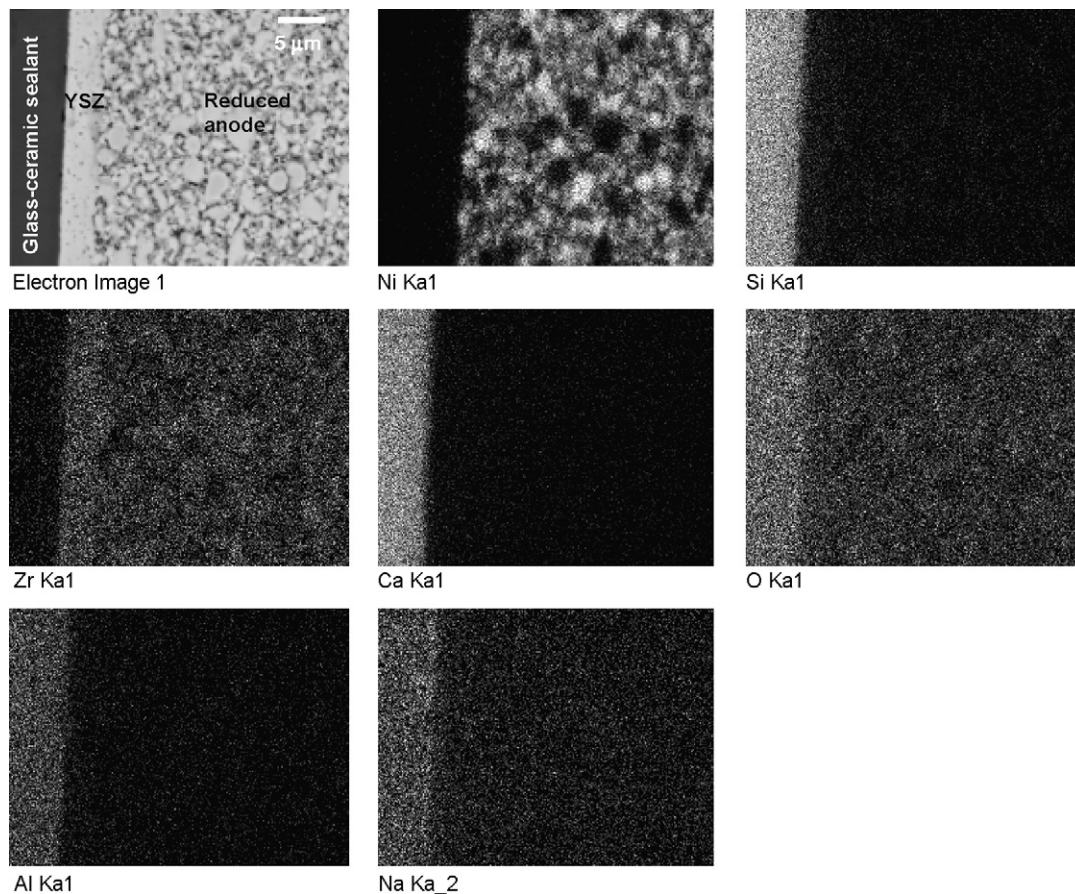


Fig. 7. EDS mapping and elements distribution at ASE/glass-ceramic sealant interface (800 °C in H₂-3% H₂O atmosphere).

tion of this sample by SEM as presented in Fig. 6 has shown a similar effect, i.e., oxidation of iron to FeO. At present there is no obvious reason as to why, contrary to chemical thermodynamic conditions, a small amount of iron oxide has been formed. Future work is being planned in order to investigate this further. The observations have confirmed that the oxidation of iron is definitely not due to reaction with the glass-ceramic sealant which has remained chemically and physically stable after undergoing treatment in the humidified hydrogen environment and there was no reaction with chromium and no sodium chromate formation which is undesirable.

Fig. 7 shows the EDS mapping and elemental distribution at the ASE/glass-ceramic interface. During the heat-treatment at 800 °C in H₂-3% H₂O atmosphere, the NiO (in the anode material) has been reduced to Ni as predicted by chemical thermodynamic data. Some porosity that was introduced by reduction of NiO to Ni can be also observed, but there are no cracks at the glass-ceramic/ASE interface. Moreover, no reactive interactions are observed between the 8YSZ and the glass-ceramic sealant after 500 h at 800 °C in H₂-3% H₂O atmosphere.

This glass-ceramic can be considered as candidate sealant between the electrolyte and the metal. In order to qualify this glass-ceramic as sealant between interconnect plates, electrical properties will be measured and provided for a follow up study in order to improve and complete the characterization on this glass-ceramic sealant.

4. Conclusions

The new glass-ceramic is a promising seal for SOFC based on Crofer22APU and ASE. The conclusions of this study are the following:

- (1) Thermal cyclic exposure of the Crofer22APU/glass-ceramic sealant and ASE/glass-ceramic sealant interfaces to air at 800 °C led to no interfacial reactions. The joints exhibited no morphological and no microstructural changes.
- (2) Continuous exposure of the Crofer22APU/glass-ceramic sealant and ASE/glass-ceramic sealant interfaces to humidified hydrogen for 500 h at 800 °C showed no interfacial products.
- (3) One of the three-phase interfacial regions was observed to exhibit a small amount of breakaway corrosion of iron to FeO which was found outside the outer layer. This observation was rather surprising because according to chemical thermodynamic calculations, the oxidation of iron is not possible under the exposure conditions that were used.
- (4) The investigation has found no evidence of any interaction between chromium and sodium oxides and no sodium chromate formation.

Acknowledgments

This work was supported in part by EU Network of Excellence project Knowledge-based Multicomponent Materials for Durable and Safe Performance (KMM-NoE, NMP3-CT-2004-502243) and MULTISS: “Design and in-house development of SOFC stacks for dealing with multiple fuels” (Regione Piemonte project, Italy). The authors are grateful to the colleagues of the Department of Energetics (Politecnico di Torino, Italy), partners of MULTISS (Regional project), that partially supported this activity.

References

- [1] B.C.H. Steele, A. Heinzl, *Nature* 414 (2001) 345–352.
- [2] R.N. Singh, *J. Appl. Ceram. Technol.* 4 (2007) 134–144.
- [3] I. Antepará, I. Villarreal, L.M. Rodríguez-Martínez, N. Lecanda, U. Castro, A. Laresgoiti, *J. Power Sources* 151 (2005) 103–107.
- [4] W.J. Fergus, *J. Power Sources* 147 (2005) 46–57.
- [5] R. Jordan, *Am. Ceram. Soc. Bull.* 87 (2008) 26–29.
- [6] K.S. Weil, *JOM* (August) (2006) 36–44.
- [7] R.N. Singh, *J. Mater. Eng. Perform.* 15 (2006) 422–426.
- [8] M. Singh, T.P. Shpargel, R. Asthana, *J. Appl. Ceram. Technol.* 4 (2007) 119–133.
- [9] J. Kim, J.S. Hardy, S. Weil, *Int. J. Hydrogen Energy* 32 (2007) 3655–3663.
- [10] L. Shiru, S. Kening, Z. Naqing, S. Yanbin, A. Maozhong, F. Qiang, Z. Xiaodong, *J. Power Sources* 168 (2007) 447–452.
- [11] Y.-S. Chou, J. Stevenson, R.N. Gow, *J. Power Sources* 168 (2007) 426–433.
- [12] Y.-S. Chou, J. Stevenson, R.N. Gow, *J. Power Sources* 170 (2007) 395–400.
- [13] M. Brochu, B.D. Gauntt, R. Shah, G. Miyake, R.E. Loehman, *J. Eur. Ceram. Soc.* 26 (2006) 3307–3313.
- [14] F. Smeacetto, M. Salvo, M. Ferraris, V. Casalegno, P. Asinari, *J. Eur. Ceram. Soc.* 28 (2008) 611–616.
- [15] S. Gosh, P. Kundu, A. Das Sharma, R.N. Basu, H.S. Maiti, *J. Eur. Ceram. Soc.* 28 (2008) 69–76.
- [16] K.D. Meinhardt, D.S. Kim, Y.-S. Chou, K.S. Weil, *J. Power Sources* 182 (2008) 188–196.
- [17] V. Kumar, A. Arora, O.P. Pandey, K. Singh, *Int. J. Hydrogen Energy* 33 (2008) 434–438.
- [18] J. Piao, K. Sun, N. Zhang, X. Chen, D. Zhou, *J. Rare Earths* 25 (2007) 434–438.
- [19] S.M. Gross, T. Koppitz, J. Rimmel, J.B. Bouche, U. Reisgen, *Fuel Cells Bull.* 9 (2006) 12–15.
- [20] Z. Yang, K.D. Meinhardt, J.W. Stevenson, *J. Electrochem. Soc.* 150 (2003) A1095–A1101.
- [21] P.H. Larsen, *J. Non-Cryst. Solids* 244 (1999) 16–24.
- [22] F. Smeacetto, M. Salvo, M. Ferraris, J. Cho, A.R. Boccaccini, *J. Eur. Ceram. Soc.* 28 (2008) 61–68.
- [23] F. Smeacetto, M. Salvo, M. Ferraris, V. Casalegno, P. Asinari, A. Chrysanthou, *J. Eur. Ceram. Soc.* 28 (2008) 2521–2527.
- [24] Z. Yang, S. Matthew, M. Walker, P. Singh, J.W. Stevenson, T. Norby, *J. Electrochem. Soc.* 151 (2004) B669–B678.
- [25] K. Ogasawara, H. Kameda, Y. Matsuzaki, T. Sakurai, T. Uehara, A. Toji, N. Sakai, K. Yamaji, T. Horita, H. Yokokawa, *J. Electrochem. Soc.* 154 (2007) B657–B663.
- [26] K.A. Nielsen, M. Solvang, S.B.L. Nielsen, A.R. Dinesen, D. Beeaff, P.H. Larsen, *J. Eur. Ceram. Soc.* 27 (2007) 1817–1822.
- [27] E.T. Turkdogan, *Physical Chemistry of High Temperature Technology*, Academic Press, New York, 1980, pp. 5–24.
- [28] E. Essuman, G.H. Meier, J. Zurek, M. Hansel, W.J. Quadackers, *Oxid. Met.* 69 (2008) 143–162.